Chapter 5. Dynamic response of a single kinocilium in a fluid velocity field

Introduction

All analysis to this point has considered the hair cell bundle to be forced by a constant point load at the tip of the kinocilium. Hair cells in many areas are attached at their tips either to the cupula or the gel layer, which makes the point load a good approximation. However, this is not always the case.

Bundles such as those on central hair cells of the cristae, the striolar region of the otolith, or the inner hair cells of the cochlea are considered, with varying degrees of confidence, to be completely free of the surrounding structure. These bundles are exposed to a large fluid filled area and are deflected by the flow of the fluid. Even if some bundles are directly attached to the gel or cupula, the presence of fluid flow may have mechanical significance providing extra force, or resistance to motion.

The remainder of this chapter will focus on the otolith organ. In the striolar area of the otolith organ, the gel layer becomes a light mesh filled with endolymph. The fluid could therefore flow (more or less) freely around the entire striola. Hair cell bundles extending into this appear to be free standing [Lim 1977]. It is theorized that these bundles are forced by fluid flow generated by the movement of the otoconial plate (see Figure 5-1).

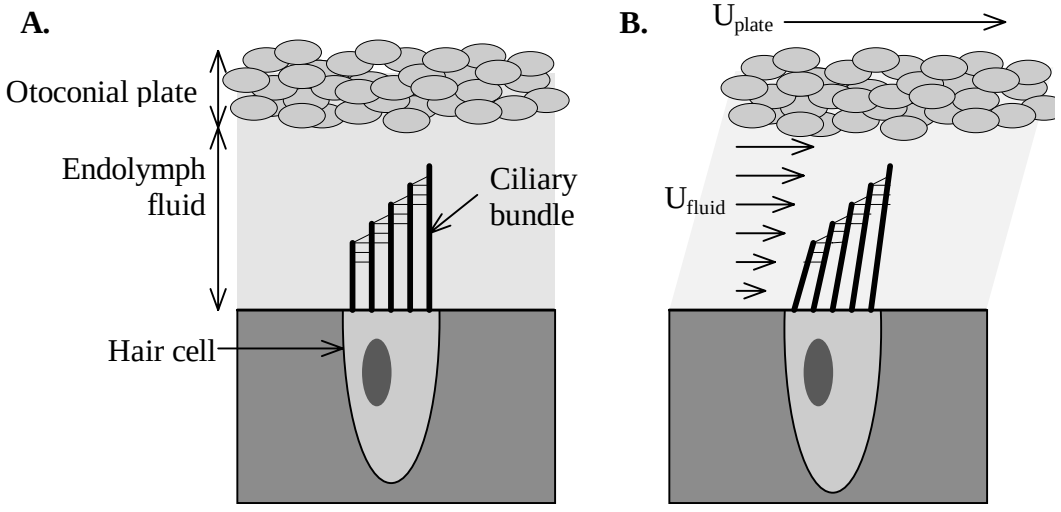

Figure 5-1. Fluid forced hair cell bundle. Part A) represents the undeformed bundle. Part B) represents how the plate's motion, via the viscous endolymph fluid, may force the bundle.

Experimental studies that observed the signals of single nerve fibers emanating from the otolith when the subject was accelerated support this hypothesis. Some recordings reflect pure acceleration while others reflect pure time rate of change of acceleration, or jerk. Most fibers

carry a signal that combines aspects of both. If the bundles are forced by fluid flow, this would seem to provide an integrating mechanism for acceleration.

This chapter is an investigation of the hypothesis that bundles in the striola are forced by fluid flow of endolymph in the striolar cavity. We wish to produce a first estimation of the response of such a system. In it, we simplify the bundle as a single kinocilium. We further assume throughout that the kinocilium is isotropic and rigidly attached to the apical surface of the hair cell. While these assumptions do not reflect biologic reality, we stress this work is a preliminary test, done to determine the influence of dominant factors such as geometry, fluid properties, as well as to test the methodolgy of performing the study. It is left to future work to determine the validity of the assumptions.

Methods

Static solution

To start, we look at the static case of a kinocilium in a constant flow of fluid. Figure 5-2 depicts our simplified model: a cantilevered beam with a circular cross section in a constant linear flow.

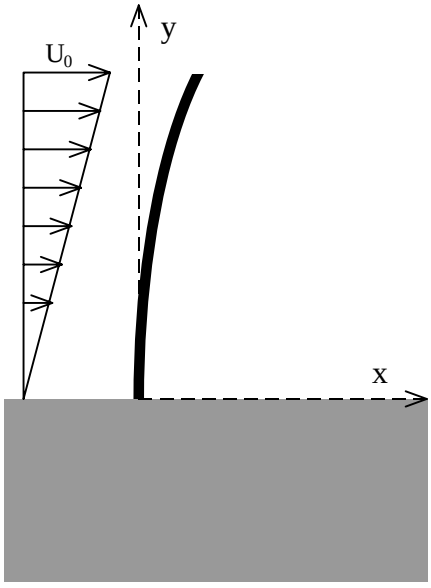

Figure 5-2. Kinocilium in linear fluid flow.

The velocity profile which increases linearly with height is defined mathematically as

$$U(y) = \frac{U_0}{l} y \qquad (5.1)$$

where U_o is the velocity at the kinocilium tip and l is the height of the kinocilium.

Next, we must determine the force acting on the kinocilium from the described fluid flow. Taking a small element of the kinocilium, as in figure 5-3

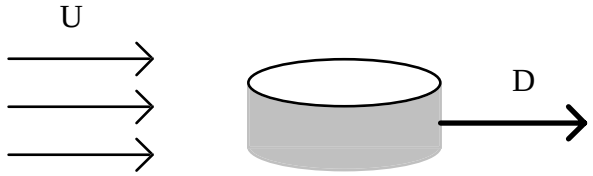

Figure 5-3. Small element of a kinocilium

the drag force,D, on a cylinder is given as:

$$D = C_D A\left(\frac{1}{2}\rho U^2\right) \tag{5.2}$$

where, A is the area normal to the fluid flow, ρ is the fluid density, U is the fluid velocity, C_D is the coefficient of drag given to be:

$$C_D = \frac{8\pi}{\mathrm{Re}\left(0.5 - \Gamma + \ln\frac{8}{\mathrm{Re}}\right)} \tag{5.3}$$

Here, Re is the Reynolds number and Γ is Euler's constant (equal to 0.577216).

The load on a differential segment of length dl at height y on the kinocilium is now defined as

$$dD = C_D d\,dl\left[\frac{1}{2}\rho U^2\right] = C_D d\,\frac{1}{2}\rho\frac{U_0^2}{l^2}y^2 dl \tag{5.4}$$

where d is the diameter of the kinocilium.

Using the classical equation for a beam in transverse loading from Euler, where our loading is taken from above, our governing equation is

$$EI\frac{d^4x}{dy^4} = \frac{C_D d\rho U_0^2}{2l^2}y^2 \tag{5.5}$$

which when solved along with boundary conditions for a cantilevered beam with no applied forces or moments at the free end gives us

$$x = \frac{C_D d\rho U_0^2}{2l^2 EI}\left[\frac{y^6}{360} - \frac{l^3 y^3}{18} + \frac{l^4 y^2}{8}\right] \tag{5.6}$$

This solution can be nondimensionalized by using the following nondimensional variables and parameters

$$\bar{y} = \frac{y}{l}$$

$$\bar{x} = \frac{x}{d}$$

$$\overline{U}_o = \frac{U_o}{d\omega} \qquad \text{(5.7a-d)}$$

$$\omega = 2\sqrt{\frac{EI}{\pi\rho d^2 l^4}}$$

to arrive at

$$\bar{x}(\bar{y}) = \frac{2}{\pi} C_D \overline{U}_o^2 \left[\frac{\bar{y}^6}{360} - \frac{\bar{y}^3}{18} + \frac{\bar{y}^2}{8} \right] \qquad \text{(5.8)}$$

The deflection profile is a quadratic with the maximum deflection seen at the tip, y=1,

$$\bar{x}(\bar{l}) = \frac{0.144}{\pi} C_D \overline{U}_o^2 \qquad \text{(5.9)}$$

Dynamic solution

Similar to the static case, the drag force on a element of kinocilium (figure 5-3) is equal to

$$D = C_D A\left(\frac{1}{2}\rho \tilde{U}\left|\tilde{U}\right|\right) \qquad \text{(5.10)}$$

Where $\tilde{U}$ is the relative difference between the velocity of the fluid and the velocity of the kinocilium, or

$$\tilde{U} = \tilde{U}(y,t) = U(y,t) - \frac{dx}{dt} \qquad \text{(5.11)}$$

It is noted that this relative difference, $\tilde{U}$, may be positive or negative, which necessitates the use of the absolute value in (5.10) rather than simply squaring the velocity term so that the drag force will always resist motion.

The forces acting on a infinitesimal section of a kinocilium are shown in figure 5-4. There is a differential drag force, dD, acting at the center and shear forces, V, at the top and bottom.

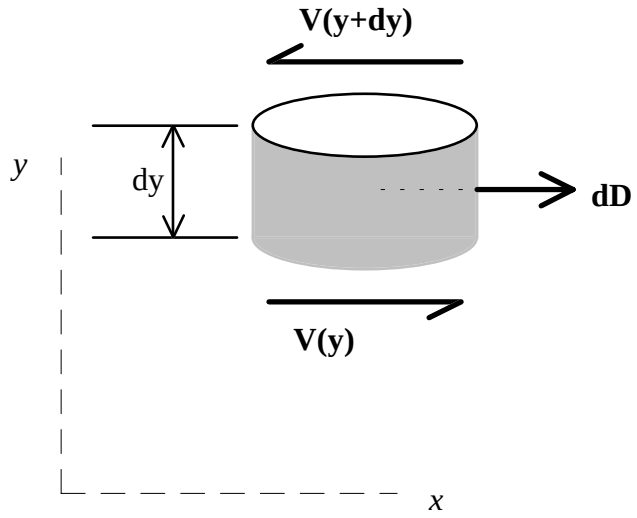

Figure 5-4. Free body diagram of a section, dy, of a kinocilium.

From Newton's first law, the equation of motion for the above section can be written

$$Ddy - \left[V(y+dy) - V(y)\right] = \rho dy A \frac{d^2x}{dt^2} \tag{5.12}$$

Upon substituting equation (5.10) for the drag force D, dividing by dy, and taking the limit as dy approaches 0, we get the differential equation

$$\frac{1}{2} C_D d\rho \left|\tilde{U}(y,t)\right| \left(\tilde{U}(y,t)\right) - \frac{dV}{dy} = \rho\pi \frac{d^2}{4} \frac{d^2x}{dt^2} \tag{5.13}$$

Finally, by substituting for the shear force as defined in Euler beam theory where

$$V = EI \frac{d^3x}{dy^3} \tag{5.14}$$

and rearranging terms, and substituting for $\tilde{U}$, we arrive at

$$EI \frac{d^4x}{dy^4} + \rho\pi \frac{d^2}{4} \frac{d^2x}{dt^2} - \frac{1}{2} C_D d\rho \left|U(y,t) - \frac{dx}{dt}\right| \left(U(y,t) - \frac{dx}{dt}\right) = 0 \tag{5.15}$$

We can nondimensionalize the above equation as in the static case, using the parameters presented in equations (5.7a-e) adding only the definition of nondimensional time as

$$\bar{t} = t\omega \tag{5.16}$$

and arrive at the dimensionless form of equation (5.15)

$$\frac{d^4\bar{x}}{d\bar{y}^4} + \frac{d^2\bar{x}}{d\bar{t}^2} - 2\frac{C_D}{\pi} \left|\bar{U}(y,t) - \frac{d\bar{x}}{d\bar{t}}\right| \left(\bar{U}(y,t) - \frac{d\bar{x}}{d\bar{t}}\right) = 0 \tag{5.17}$$

We immediately notice the first and second terms have coefficients of the magnitude of 10^0. The third term is the forcing function, and is nonlinear.

Fluid velocity

The static solution assumed a linear flow, while the dynamic solution assumed the flow was a function of height and time. To flesh out the latter, I investigated the possible fluid flow generated by the striolar cavity. Earlier work [Grant, 1997] has described the displacement of the otoconial layer when the organ experiences a step change in acceleration as

$$\delta = \delta_{\max}\left(1 - e^{-t/\tau}\right) \tag{5.18}$$

where δ_{max} is the maximum deflection of the layer and τ is an experimentally determined time constant. Therefore the velocity of the plate is the derivative of displacement with respect to time, or

$$V_p = \frac{d\delta}{dt} = \frac{\delta_{\max}}{\tau} e^{-t/\tau} = V_{p-\max} e^{-t/\tau} \tag{5.19}$$

Now, by inspecting the geometry of the striolar region of the utricle we simplify the problem into a one dimensional problem (figure 5-5). This is the Stokes problem familiar in viscous fluid flow. In it we have a fluid between two plates which undergo changes in position with respect to time.

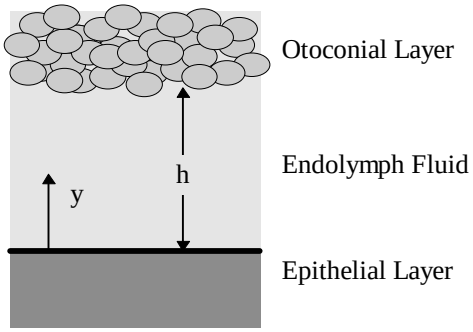

Figure 5-5. Geometry for the fluid flow problem. Variations in velocity are only seen in the vertical (y) direction.

The velocity of the fluid, u(y,t), is a function of time and one spatial dimension, y. The relationship between these values is described by the one dimensional, no pressure gradient Navier Stokes equation,

$$\frac{du}{dt} = \nu \frac{d^2 u}{dy^2} \tag{5.20}$$

where ν is the kinematic viscosity of the fluid, defined as

$$\nu = \frac{\mu}{\rho}. \tag{5.21}$$

The boundary conditions for this problem are chosen to reflect the no-slip conditions with the two plates, thus

$$u(0,t) = 0$$
$$u(h,t) = V_p = V_{p-\max} e^{-t/\tau} \qquad (5.22a,b)$$

To this is added the initial condition of the endolymph fluid being at rest

$$u(y,0) = 0\,. \qquad (5.23)$$

As before, the above equations will be nondimensionalized using the same variables as before for time, velocity (although here the velocity pertains to the fluid), and length.

$$\bar{t} = t\omega$$
$$\bar{u} = \frac{u}{d\omega} \qquad (5.24a\text{-}c)$$
$$\bar{y} = \frac{y}{l}$$

Parameters are nondimensionalized as follows.

$$\bar{h} = \frac{h}{l}$$
$$\bar{\delta}_{\max} = \frac{\delta_{\max}}{d}$$
$$\bar{\tau} = \tau\omega \qquad (5.25a\text{-}e)$$
$$\bar{V}_{p-\max} = \frac{V_{p-\max}}{d\omega}$$
$$\bar{\nu} = \frac{\nu}{l^2\omega}$$

The nondimensional equation for the fluid flow is then

$$\frac{d\bar{u}}{d\bar{t}} = \bar{\nu}\frac{d^2\bar{u}}{d\bar{y}^2} \qquad (5.26)$$

with boundary conditions

$$\bar{u}(0,\bar{t}) = 0$$
$$\bar{u}(\bar{h},\bar{t}) = \bar{V}_p = \bar{V}_{p-\max} e^{-\bar{t}/\bar{\tau}} \qquad (5.27a,b)$$

and initial condition

$$\bar{u}(\bar{y},0) = 0\,. \qquad (5.28)$$

Finite difference techniques

To solve the equations for both the kinocilium and fluid motion, I utilized finite difference techniques. All subsequent equations will drop the overbars, but imply the use of dimensionless units.

Equations for the kinocilium

For computational convenience, I converted the one-variable, fourth-order equation (5.17) into two second-order equations, with two variables S, the nondimensional shear, and V, the nondimensional velocity, defined as

$$S = \frac{d^2x}{dy^2} \quad V = \frac{dx}{dt} \tag{5.28}$$

The simultaneous governing equations for the kinocilium are now

$$\begin{cases} \dfrac{dS}{dt} - \dfrac{d^2V}{dy^2} = 0 \\ \dfrac{d^2S}{dy^2} + \dfrac{dV}{dt} - \dfrac{2C_d}{\pi}|U-V|(U-V) = 0 \end{cases} \tag{5.29}$$

where the first equation is derived from (5.28) and the second is from (5.17).

I add boundary conditions of no motion at the base and no applied force or moment at the tip

$$\begin{aligned} &V(0,t) = 0 \\ &\frac{dV(0,t)}{dy} = 0 \\ &S(1,t) = 0 \\ &\frac{dS(1,t)}{dy} = 0 \end{aligned} \tag{5.30a-d}$$

and initial conditions of

$$\begin{aligned} &S(y,0) = \frac{d^2x_o(y)}{dy^2} \\ &V(y,0) = V_o(y) \end{aligned} \tag{5.31a,b}$$

The kinocilium was divided into M equal pieces, denoted by M+1 nodal points. Finite difference analogues to derivatives were used to represent the spatial derivatives in the two governing equations. Specifically, the second derivative with respect to space is

$$\frac{d^2x}{dy^2} = \frac{x_{i+1,n} - 2x_{i,n} + x_{i-1,n}}{\Delta y^2} + O(\Delta y^2) \tag{5.32}$$

where x represents use as both shear, S, and velocity, V.

Because of the nonlinear nature of the governing equations, an explicit method was used to step forward in time. Starting from the known initial conditions, the solution at successive times was obtained by advancing at small increments, Δt. Therefore, the finite difference analogue for the first derivative with respect to time is

$$\frac{dx}{dt} = \frac{x_{i,n+1} - x_{i,n}}{\Delta t} + O(\Delta t) \tag{5.33}$$

The two-dimensional (one dimension in space and one in time) solution space can be visualized in figure 5-5.

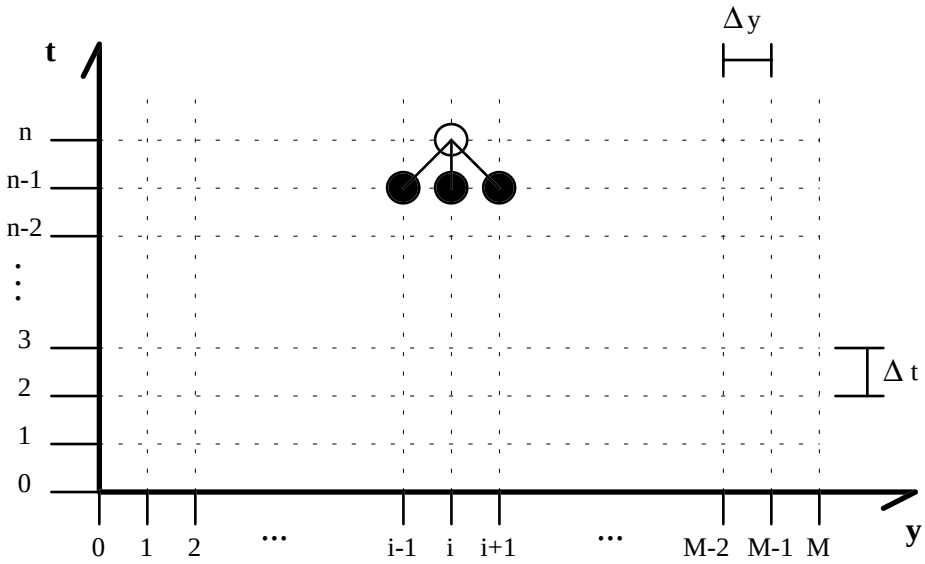

Figure 5-6. Solution space for dynamic kinocilia problem. White circle at point t=n and y=i is directly determined by the values at positions shown by the black circles.

The finite difference analogues were substituted into the two governing equations (5.29) and solved for the unknowns, S_{n+1} and V_{n+1}. For the interior of the solution space (I = 1, M-1) the following equations were used.

$$S_{i,n+1} = \frac{\Delta t}{\Delta y^2}\left[V_{i+1,n} - 2V_{i,n} + V_{i-1,n}\right] + S_{i,n}$$

$$V_{i,n+1} = -\frac{\Delta t}{\Delta y^2}\left[S_{i+1,n} - 2S_{i,n} + S_{i-1,n}\right] + 2\frac{C_D}{\pi}\Delta t\left|U(y,t) - V_{i,n}\right|\left[U(y,t) - V_{i,n}\right] + V_{i,n} \qquad (5.34a,b)$$

To obtain displacement, x, a simple integration with respect to time was used on the value of velocity, V,

$$x_{i,n+1} = x_{i,n} + \frac{\Delta t}{2}\left[V_{i,n+1} + V_{i,n}\right] + O(\Delta t)^2 \qquad (5.35)$$

The imposition of the boundary conditions of the equation are worthy of remark. At node 1, $V_{0,n} = 0$, which is easy enough to use. Additionally, at that position,

$$\left.\frac{dV}{dy}\right|_{o,n} = \frac{V_{2,n} + V_{0,n}}{2\Delta y} + O(\Delta y)^2 = 0 \qquad (5.36)$$

Which leads to

$$V_{o,n} = V_{2,n} - 2\Delta y\left.\frac{dV}{dy}\right|_{0,n} = V_{2,n} \qquad (5.37)$$

Which, when applied to eq. (5.22a) at node I=1, leads to

$$S_{1,n+1} = 2\frac{\Delta t}{\Delta y^2}\left[V_{2,n} - V_{1,n}\right] + S_{i,n} \tag{5.38}$$

At node M, we have $S_{M,n} = 0$, as well as

$$\left.\frac{dS}{dy}\right|_{M,n} = \frac{S_{M+1,n} - S_{M-1,n}}{2\Delta y} + O(\Delta y)^2 \tag{5.39}$$

which leads to

$$S_{M+1,n} = S_{M-1,n} + 2\Delta y \left.\frac{dS}{dy}\right|_{M,n} = S_{M-1,n} \tag{5.40}$$

Which when applied to equation (5.22b) at node M, leads to

$$V_{M,n+1} = 2\frac{\Delta t}{\Delta y^2}\left[S_{M,n} - S_{M-1,n}\right] + \frac{2C_d}{\pi}\Delta t\left[U(y,t) - V_{M,n}\right]\left|U(y,t) - V_{M,n}\right| + V_{M,n} \tag{5.41}$$

The above equations were coded into Fortran and solved on a Silicon Graphics Indigo[2].

Equations for fluid flow

For cases where the fluid profile was not known equations (5.26), (5.27), and (5.28) must be solved to input to the above equations. Since I solve for the displacement of the kinocilium using a finite difference technique, it is a simple matter (relatively speaking, of course) to define a nodal variable for fluid velocity, $u_{i,n}$, and solve the fluid problem simultaneously with the dynamic beam problem presented above.

By using finite difference analogues of the derivatives, the fluid governing equation (5.26) is transformed into

$$\frac{u_{i,n+1} - u_{i,n}}{\Delta t} = \nu\frac{u_{i+1,n} - 2u_{i,n} + u_{i-1,n}}{\Delta y^2} \tag{5.42}$$

which using algebra to solve for times, t = n+1, leads to the explicit formula

$$u_{i,n+1} = \frac{\Delta t}{\Delta y^2}\nu u_{i+1,n} - \left[2\frac{\Delta t}{\Delta y^2}\nu - 1\right]u_{i,n} + \frac{\Delta t}{\Delta y^2}\nu u_{i-1,n} \tag{5.43}$$

Notable is the fact that the fluid velocity may vary so much that a constant value for the drag coefficient C_D is no longer valid. It is a simple matter to recalculate C_D at every time step, at every node based upon the fluid velocity.

The solution algorithm then becomes,

- solve for the fluid velocity at each node,
- solve for kinocilium velocity and bending,
- solve for kinocilium displacement,
- step forward one time step and solve again.

Results

Realistic Parameters

To use the above equations in our model, as well as to draw any conclusions about the response of hair cell bundles, I need to put some values in for the parameters. Some of these are intended to be rough estimates, while others are quite well established.

To start, the physical dimensions of the problem will be stated as follows:

- kinocilium height is 10 microns
- kinocilium diameter is 0.2 microns
- distance from apical surface to otoconial plate 30 microns

Material properties of the system include

- Young's modulus for kinocilium 1 x 10^9 N/m^2
- Endolymph fluid viscosity is 0.1 centipoise
- Endolymph density is 10^3 kg/m^3

According to Grant [1997], the parameters describing plate motion are

- δ_{max} can be small to around 30 microns
- τ is 0.01 seconds

Immediate implications of the above the maximum fluid velocity at the otoconial plate is 3 x 10^{-3} m/s. Assuming the fluid below reaches steady flow, with a corresponding linear flow, the maximum fluid velocity at the kinocilium tip is one third of that or 10^{-3} m/s.

The Reynold's number for the system, defined as

$$\mathrm{Re} = 2\frac{Ud}{\nu} \qquad (5.44)$$

is then a maximum of 4 x 10^{-6}, with values being less than that for situations with the flow less than maximum and when the kinocilium is moving with the flow. This obviously is a very viscous problem.

Static case results

To start, examination of the static deflection will be done. This will be done using the parameters presented in the previous section, including the maximum fluid velocity. From equation (5.9) the static deflection at the tip reaches a maximum of 2 times the diameter. Redimensionalizing the results of (5.9) shows maximum deflection to be 0.4 microns.

Fluid added

For the solution, the kinocilium was broken into 21 nodes and the fluid field 61 nodes with step sizes of the same height. The solution converged with a time step size of 10^{-4} nondimensional time units. Results are plotted for both the displacement and the velocity of the kinocilium tip and the fluid velocity at the kinocilium tip height in figures (5.6) and (5.7) below.

The tip displacement follows a smooth curve to it's maximum displacement, before decaying as the plate itself slows down.

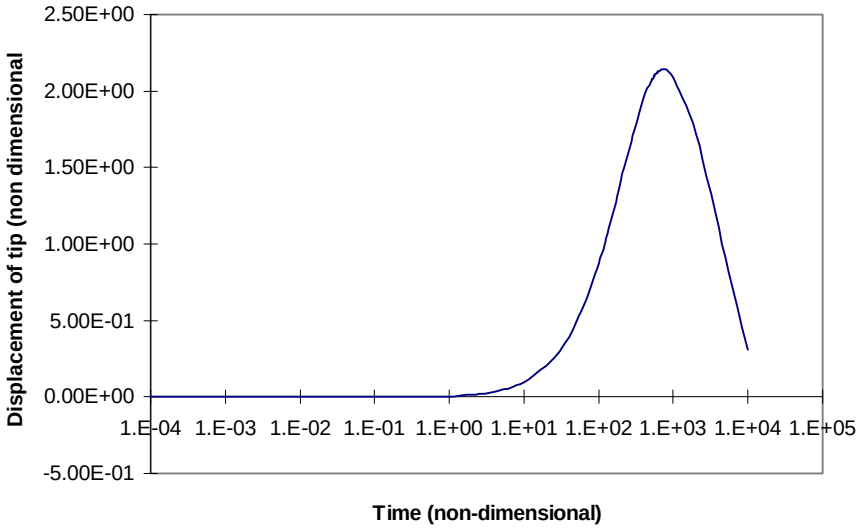

Figure 5-7. Displacement of the kinocilium tip.

The fluid velocity attained a linear profile, within 1 nondimensional second. The kinocilium tip also followed the fluid velocity at that height. Soon however, the kinocilium reached the equilibrium between its own stiffness and the fluid drag, its velocity decreased. As the plate velocity decayed the fluid velocity began to drop.

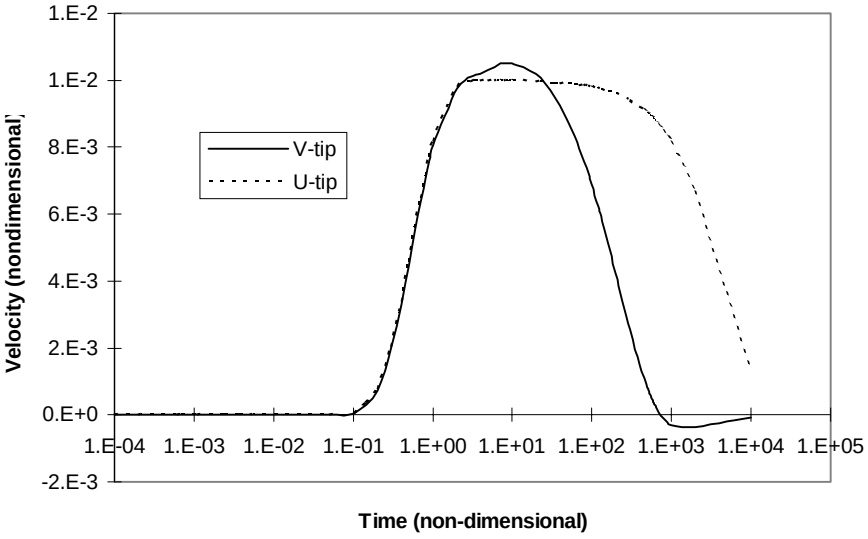

Figure 5-8. Fluid and kinocilium velocity at tip for plate problem.

Discussion

Upon redimensionalization, we see the kinocilium has a response time of about 10^{-3} sec. Hair cell bundles have a response of at least milliseconds (10^{-3} sec) [Grant, 1997], which does not preclude the possibility of fluid forcing as a mechanism for coupling cupular or gel layer deflection to the hair cell bundle.

Conclusions

This study is a preliminary effort. Future work may need to include a more comprehensive model of fluid flow, including the effect of the entire bundle, and a more biologic representation of the cilia.